Absolute Reactivity of the 4-Methoxycumyl Cation in Non-Acid Zeolites

Melanie A. O'Neill, Frances L. Cozens,* and Norman P. Schepp

Contribution from the Department of Chemistry, Dalhousie University, Halifax, Nova Scotia, Canada B3H 4J3

Received October 8, 1999

Abstract: The reactivity of the 4-methoxycumyl cation in a series of alkali metal cation-exchanged zeolites (LiY, NaY, KY, RbY CsY, NaX, NaMor, and Naβ) in the absence and presence of coadsorbed alcohols and water is examined using nanosecond laser flash photolysis. In dry zeolites, the absolute reactivity of the carbocation is found to be strongly dependent on the nature of the alkali counterion, the Si/Al ratio, and the framework morphology, with the lifetime of the carbocation in Naβ being almost 10000-fold longer than in CsY. The results suggest a mechanism for carbocation decay involving direct participation of the zeolite framework as a nucleophile, leading to the generation of a framework-bound alkoxy species. Intrazeolite addition reactions of alcohols and water to the 4-methoxycumyl cation can be described in terms of both dynamic and static quenching involving molecular diffusion through the heterogeneous topology and rapid coupling between the alcohol and the carbocation encapsulated within the same cavity. The dynamics of the quenching reactions are different from similar reactions in homogeneous solution due to both the passive and active influences of the zeolite environment. In a passive sense, the zeolite decreases the reactivity of the nucleophilic quencher by hindering molecular diffusion. However, the zeolite actively promotes the efficiency of intracavity coupling by enhancing the deprotonation of the oxonium ion intermediate, allowing the reaction to go to completion.

Introduction

Studies of intrazeolite reaction dynamics continue to improve our understanding of host−guest interactions and the role that zeolites play in the mechanisms and kinetics of photochemical and thermal transformations.[1−11] Zeolites are microporous crystalline aluminosilicate materials constructed of $[SiO_4]^{4-}$ and $[AlO_4]^{5-}$ tetrahedra where every aluminum present in the framework results in a net negative charge that must be balanced with an exchangeable cation.[12−15] The geometry of the open framework structure leads to an interesting architecture with an array of molecular-sized pores, channels, and cavities of various shapes and sizes depending on the morphology of the zeolite. This anionic network of well-defined void spaces and associated counter-balancing cations generates a polar matrix with localized electrostatic fields and active acidic and basic sites. As a result, there has been considerable interest in the ability of these solid materials to modify and/or promote a variety of fundamental reactions in organic chemistry.[16−28]

In particular, much effort has been directed toward understanding the chemistry of carbocations generated within the channels and cavities of zeolites. These studies have generally been restricted to carbocations produced in proton-exchanged Brønsted zeolites,[7,11,29−45] or zeolites with divalent metal ions

(1) Turro, N. J. *Pure Appl. Chem.* **1986**, *58*, 1219−1228.
(2) Ramamurthy, V.; Turro, N. J. *J. Inclusion Phenom. Mol. Recognit. Chem.* **1995**, *21*, 239−282.
(3) Ramamurthy, V. In *Photochemistry in Organized and Constrained Media*; Ramamurthy, V., Ed.; VCH: New York, 1991; pp 429−493.
(4) Weiss, R. G.; Ramamurthy, V.; Hammond, G. S. *Acc. Chem. Res.* **1993**, *26*, 530−536.
(5) Ramamurthy, V.; Eaton, D. F.; Caspar, J. V. *Acc. Chem. Res.* **1992**, *25*, 299−307.
(6) Dutta, P. K. *J. Inclusion Phenom. Mol. Recognit. Chem.* **1995**, *21*, 215−237.
(7) Corma, A. *Chem. Rev.* **1995**, *95*, 559−614.
(8) Thomas, J. K. *Chem. Rev.* **1993**, *93*, 301−320.
(9) Yoon, K. B. *Chem. Rev.* **1993**, *93*, 321−339.
(10) Hattori, H. *Chem. Rev.* **1995**, *95*, 537−558.
(11) Kiricsi, I.; Horst, F.; Tasi, G.; Nagy, J. B. *Chem. Rev.* **1999**, *99*, 2085−2114.
(12) Breck, D. W. *J. Chem. Educ.* **1964**, *41*, 678−689.
(13) Breck, D. W. *Zeolite Molecular Sieves: Structure, Chemistry and Use*; John Wiley and Sons: New York, 1974.
(14) Dyer, A. *An Introduction to Zeolite Molecular Sieves*; John Wiley and Sons: Bath, 1988.
(15) van Bekkum, H.; Flanigen, E. M.; Jansen, J. C. *Introduction to Zeolite Science and Practice*: Elsevier: Amsterdam and New York, 1991.
(16) Alvaro, M.; Garcia, H.; Garcia, S.; Marquez, F.; Scaiano, J. C. *J. Phys. Chem. B* **1997**, *101*, 3043−3051.
(17) Corma, A.; Fornes, V.; Garcia, H.; Marti, V.; Miranda, M. A. *Chem. Mater.* **1995**, *7*, 2136−2143.
(18) Baldovi, M. V.; Cozens, F. L.; Fornes, V.; Garcia, H.; Scaiano, J. C. *Chem. Mater.* **1996**, *8*, 152−160.
(19) Cozens, F. L.; Regimbald, M.; Garica, H.; Scaiano, J. C. *J. Phys. Chem.* **1996**, *100*, 18165−18172.
(20) Cozens, F. L.; Cano, M. L.; Garcia, H.; Schepp, N. P. *J. Am. Chem. Soc.* **1998**, *120*, 5667−5673.
(21) Ramamurthy, V.; Lakshminarasimhan, P.; Grey, C. P.; Johnston, L. J. *Chem. Commun.* **1998**, 2411−2425.
(22) Brancaleon, L.; Brousmiche, D.; Rao, V. J.; Johnston, L. J.; Ramamurthy, V. *J. Am. Chem. Soc.* **1998**, *120*, 4926−4933.
(23) Turro, N. J.; Lei, X.; Li, W.; McDermott, A.; Abrams, L.; Ottavianai, M. F.; Beard, H. S. *Chem. Commun.* **1998**, 695−696.
(24) Turro, N. J.; McDermott, A.; Lei, X.; Li, W.; Abrams, L.; Ottavianai, M. F.; Beard, H. S.; Houk, K. N.; Beno, B. R.; Lee, P. S. *Chem. Commun.* **1998**, 697−698.
(25) Yoon, K. B.; Park, Y. S.; Kochi, J. K. *J. Am. Chem. Soc.* **1996**, *118*, 12710−12718.
(26) Yoon, K. B.; Hubig, S. M.; Kochi, J. K. *J. Phys. Chem.* **1994**, *98*, 3865−3871.
(27) Liu, X.; Iu, K.; Thomas, J. K. *J. Phys. Chem.* **1994**, *98*, 7877−7884.
(28) Hashimoto, S. *J. Chem. Soc., Faraday Trans.* **1997**, *93*, 4401−4408.
(29) Corma, A.; Garcia, H. *Top. Catal.* **1998**, 127−140.
(30) Cano, M. L.; Corma, A.; Fornes, V.; Garcia, H.; Miranda, M. A.; Baerlocher, C.; Lengauer, C. *J. Am. Chem. Soc.* **1996**, *118*, 11006−11013.

10.1021/ja993619d CCC: $19.00
Published on Web 06/08/2000

such as Ca^{2+} that also contain Brønsted acid sites upon thermal activation.[46−49] This is primarily due to the fact that in the highly acidic environment provided by acid zeolites, carbocations are easily generated and, more importantly, are thermodynamically stabilized to the extent that they can be readily examined by steady-state techniques such as solid-state NMR,[38−41] UV−vis diffuse reflectance,[29−37] and UV−vis absorption spectroscopy.[42,43]

While tremendous advances in our understanding of the effect of zeolite structure and morphology on the chemistry of carbocations have been made from studies in acid zeolites, studies using nonprotic alkali metal cation-exchanged zeolites would be extremely useful in providing further insights into the nature of the interactions between the zeolite framework and the embedded carbocation. For example, the effect of properties such as electrostatic field strength and cation size on the chemistry of carbocations located within zeolite cavities can be readily examined using alkali metal exchanged zeolites, but not with Brønsted-acid zeolites, simply by looking at the behavior of carbocations as a function of different exchangeable counterions. Furthermore, the [Si−O−Al] bridges in nonprotic cation-exchanged zeolites have distinctly enhanced Lewis base (i.e. nucleophilic) activity that is expected to be strongly dependent on the nature of the counterion. Thus, the possibility that reactions of unstable carbocations within zeolites involve a direct interaction between the anionic sites on the framework and the carbocation to generate framework bound alkoxy species can be explored with alkali metal cation-exchanged zeolites by looking at the absolute reactivity of the carbocation as a function of the nature of the charge balancing cation. In addition, nonprotic cation-exchanged zeolites are suitable media for determining the dynamics of second-order reactions of co-incorporated nucleophiles with carbocations. These reactions are difficult to study in Brønsted zeolites due to the reversible addition of nucleophiles such as water and alcohols in the highly acidic environment, as well as the probability that the nucleophilicity of many common nucleophiles will be considerably reduced by protonation. In addition, the stability of some nucleophiles like alkenes will be low within the strongly acidic environment of the proton-exchanged zeolites.

To address these issues, we have recently developed a method to generate reactive carbocations within nonprotic cation-exchanged zeolites.[50] With this technique, we can now examine the reactivity of carbocations in various zeolite environments. As well, the dynamics and mechanisms for the addition of nucleophiles such as alcohols can be investigated without having to take into account problems associated with the protonation state and stability of the nucleophile. In the present work, we describe results concerning the effect of the alkali metal counterion, aluminum content, and framework morphology on the absolute reactivity of the 4-methoxycumyl cation embedded within the cavities of cation-exchanged zeolites. Our results demonstrate for the first time that the carbocation lifetime is indeed strongly influenced by the nature, and in particular the nucleophilicity, of the active site within these alkali metal cation-exchanged zeolites. We also address questions concerning the effect of zeolite composition on the rate constant for bimolecular reactions of carbocations with alcohol nucleophiles within the zeolite lattice.

Results

Formation of the 4-Methoxycumyl Cation in Dry Alkali Metal Cation-Exchanged Zeolites. Laser photolysis of 4,4′-dimethoxybicumene incorporated within the cavities of NaY under vacuum (10^{-3} Torr) conditions leads to the formation of the 4-methoxycumyl cation, $\lambda_{max} = 360$ nm.[50,51] The 4-methoxycumyl cation is formed via rapid fragmentation of the 4,4′-dimethoxybicumene radical cation[52−54] that is generated upon laser-induced photoionization of zeolite-encapsulated 4,4′-dimethoxybicumene, eq 1.[50] The same laser-initiated photoreaction readily generates the 4-methoxycumyl cation within other alkali metal cation-exchanged Y zeolites (LiY, KY, RbY, and CsY), and within zeolites that differ in their Si/Al ratio and framework morphology (NaX, Si/Al = 1.2; NaMordenite, Si/Al = 6.5; and Naβ, Si/Al = 18), Table 1. In each case, the transient diffuse reflectance spectrum is dominated by the presence of a strong absorption band centered at 360 nm, Figure 1, which is the known absorption maximum for the 4-methoxycumyl cation, that behaves in a manner consistent with the formation of the carbocation. In particular, the transient species is not affected by the addition of molecular oxygen, but decays more rapidly in the presence of nucleophiles such as water and alcohols (vide infra). The possibility that the transient is the 4,4′-dimethoxybicumene radical cation can be ruled out as

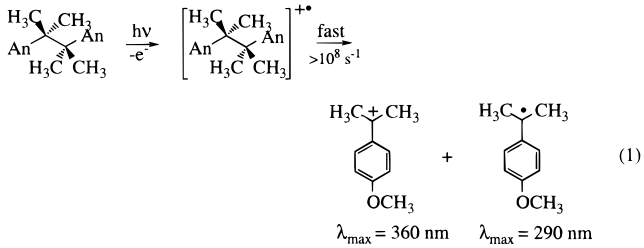

(1)

(31) Cano, M. L.; Cozens, F. L.; Fornes, V.; Garcia, H.; Scaiano, J. C. *J. Phys. Chem.* **1996**, *100*, 18145−18151.
(32) Cano, M. L.; Cozens, F. L.; Garcia, H.; Vicente, M.; Scaiano, J. C. *J. Phys. Chem.* **1996**, *100*, 18152−18157.
(33) Garcia, H.; Garcia, S.; Perez-Prieto, J.; Scaiano, J. C. *J. Phys. Chem.* **1996**, *100*, 18158−18164.
(34) Cozens, F. L.; Garcia, H.; Scaiano, J. C. *Langmuir* **1994**, *10*, 2246−2249.
(35) Cozens, F. L.; Garcia, H.; Scaiano, J. C. *J. Am. Chem. Soc.* **1993**, *115*, 11134−11140.
(36) Cozens, F. L.; Bogdanov, R.; Regimbald, M.; Garcia, H.; Marti, V.; Scaiano, J. C. *J. Phys. Chem. B* **1997**, *101*, 6821−6829.
(37) Liu, X. L.; Iu, K.; Thomas, J. K.; He, H.; Klinowski, J. *J. Am. Chem. Soc.* **1994**, *116*, 118111−11811.
(38) Nicholas, J. B.; Haw, J. F. *J. Am. Chem. Soc.* **1998**, *120*, 11804−11805.
(39) Xu, T.; Barich, D. H.; Goguen, P. W.; Song, W.; Wang, Z.; Nicholas, J. B.; Haw, J. F. *J. Am. Chem. Soc.* **1998**, *120*, 4025−4026.
(40) Haw, J. F.; Nicholas, J. B.; Xu, T.; Beck, L. W.; Ferguson, D. B. *Acc. Chem. Res.* **1996**, *29*, 259−267.
(41) Tao, T.; Maciel, G. E. *J. Am. Chem. Soc.* **1995**, *117*, 12889−12890.
(42) Kiricsi, I.; Tasi, G.; Fejes, P.; Forster, H. *J. Chem. Soc., Faraday Trans.* **1993**, *89*, 4221−4224.
(43) Forster, H.; Kiricsi, I.; Hannus, I. *J. Mol. Struct.* **1993**, *296*, 61−67.
(44) van Santen, R. A.; Kramer, G. J. *Chem. Rev.* **1995**, *95*, 637−660.
(45) Kazansky, V. B. *Acc. Chem. Res.* **1991**, *24*, 379−383.
(46) Kao, H.; Grey, C. P.; Pitchumani, K.; Lakshminarasimhan, P. H.; Ramamurthy, V. *J. Phys. Chem. A* **1998**, *102*, 5627−5639.
(47) Pitchumani, K.; Joy, A.; Prevost, N.; Ramamurthy, V. *Chem. Commun.* **1997**, 127−128.
(48) Pitchumani, K.; Lakshminarasimhan, P. H.; Turner, G.; Bakker, M. G.; Ramamurthy, V. *Tetrahedron Lett.* **1997**, *38*, 371−374.
(49) Pitchumani, K.; Ramamurthy, V. *Chem. Commun.* **1996**, 2763−2764.
(50) Cozens, F. L.; O'Neill, M.; Schepp, N. *J. Am. Chem. Soc.* **1997**, *119*, 7583−7584.
(51) McClelland, R. A.; Chan, R. A.; Cozens, F. L.; Modro, A.; Steenken, S. *Angew. Chem., Int. Ed. Engl.* **1991**, *30*, 1337−1339.
(52) Maslak, P.; Chapman, W. H., Jr. *J. Org. Chem.* **1996**, *61*, 2647−2656.
(53) Maslak, P. *Top. Curr. Chem.* **1993**, *168*, 1−65.
(54) Maslak, P.; Chapman, W. H., Jr. *Tetrahedron* **1990**, *46*, 2715−2724.

Table 1. Description of Zeolites Used in the Present Study

zeolite	Si/Al	counterion	pore diameter/Å	channel system/cage diameter
Faujasite Y	2.4	alkali M^{+a}	7.4	3-D channel with cage/13 Å
Faujasite X	1.2	Na^+	7.4	3-D channel with cage/13 Å
β	18	Na^+	7.6 × 6.4; 5.5 × 5.5	tridirectional channel system
Mordenite	6.5	Na^+	6.5 × 7.0; 2.6 × 5.7	unidirectional channel system

[a] $M^+ = Li^+, Na^+, K^+, Rb^+, Cs^+$.

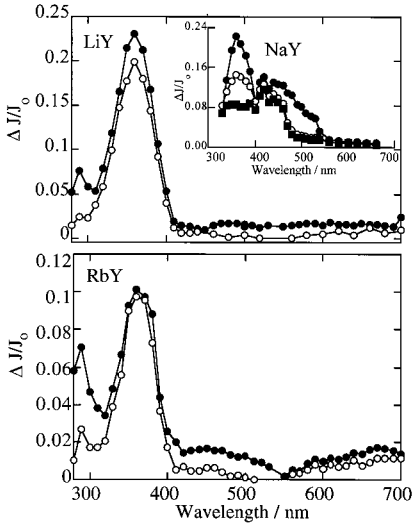

Figure 1. Transient diffuse reflectance spectra generated 320 ns after 266-nm laser irradiation of 4,4′-dimethoxybicumene in LiY and RbY under vacuum (10^{-3} Torr) (closed circles) and oxygen (open circles) conditions. The insert shows the transient diffuse reflectance spectrum generated upon 308-nm laser irradiation of chloranil in NaY with 4,4′-dimethoxybicumene under vacuum (10^{-3} Torr) conditions. The spectra were taken 400 ns (closed circles), 3.32 μs (open circles), and 13.6 μs (closed squares) after the laser pulse.

substituted anisole radical cations such as that of 4-methoxytoluene have absorption maxima near 420 nm in both solution[55] and zeolites,[56] and these radical cations are not quenched by nucleophiles such as alcohols (vide infra). In fact, our inability to observe the radical cation on the nanosecond time scale was expected, since previous studies have shown that the 4,4′-dimethoxybicumene radical cation fragments in solution to give the carbocation and the radical with a rate constant of ca. 10^8 s^{-1}.[52,53]

A band at 290 nm is also observed in the time-resolved diffuse reflectance spectra (Figure 1). The decay of this band is much slower than the decay of the carbocation at 360 nm, indicating the presence of a second transient species upon laser irradiation of 4,4′-dimethoxybicumene. Unlike the carbocation band at 360 nm, the band at 290 nm is efficiently quenched by the presence of molecular oxygen within the zeolite framework. We assign this band to the 4-methoxycumyl radical produced as the second fragmentation product upon cleavage of the 4,4′-dimethoxybicumene radical cation, eq 1. Quenching of the transient by oxygen and the location of the absorption maximum at 290 nm are in agreement with this assignment.[57] In addition, the relatively long lifetime of this transient species is consistent with that demonstrated for similar zeolite-encapsulated benzylic radicals.[58]

Further evidence for the mechanism of carbocation formation comes from experiments carried out with a co-incorporated photoinduced electron-transfer sensitizer. Figure 1 (insert) shows the transient diffuse reflectance spectrum obtained upon 308-nm laser photolysis of chloranil in the presence of 4,4′-dimethoxybicumene in NaY under vacuum conditions, eq 2.

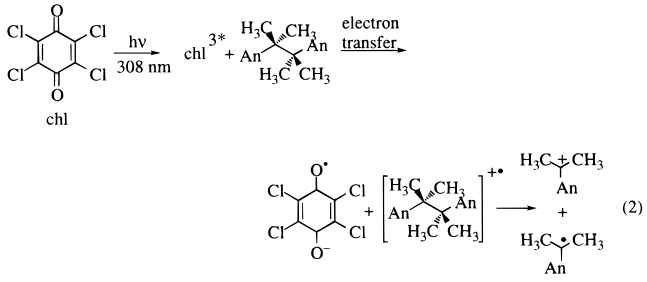

(2)

The spectrum clearly shows the presence of the 4-methoxycumyl cation located at 360 nm, as well as bands at 420 and 450 nm due to the chloranil radical anion.[59,60] A short-lived weak band at 500 nm due to the chloranil triplet[60,61] is also observed under vacuum conditions. Observation of the carbocation under these photoinduced electron transfer conditions directly supports the conclusion that the carbocation is produced by rapid fragmentation of the radical cation formed by photoionization of the precursor in the absence of the sensitizer, eq 1.

Absolute Reactivity of the 4-Methoxycumyl Cation in Y Zeolites. The absolute reactivity of the 4-methoxycumyl cation in the various dry cation-exchanged zeolites was measured by monitoring the intensity of the reflectance at 360 nm as a function of time using nanosecond time-resolved diffuse reflectance. To get an accurate picture of the decay profile of the carbocation within the heterogeneous environment of each zeolite, kinetic decay traces obtained over several different time scales were combined to generate stretched exponential traces that represent the disappearance of the carbocation over several decades.[62] Stretched decay traces for the 4-methoxycumyl cation within the zeolites with varying charge balancing cations, Si/Al ratios, and framework topologies are shown in Figure 2. The stretched decay profiles were analyzed using the exponential series method[63] to account for the possibility that the carbocation might decay with a broad distribution of lifetimes. However, these calculations gave a surprisingly narrow range of lifetimes evenly distributed about one or two central values, Figure 2 inset, indicating that the decay of the 4-methoxycumyl cation within these zeolites is made up of only one or two first-order processes.[63] Thus, the decay traces were fit to either a single or double first-order equation as required. In LiY, the decay trace fit well to a consecutive first-order exponential equation to give

(55) Baciocchi, E.; Del Giacco, T.; Elisei, F. *J. Am. Chem. Soc.* **1993**, *115*, 12290−12295.
(56) Supporting Information: see paragraph at the end of this paper regarding availability.
(57) Tokumura, K.; Ozaki, T.; Nosaka, H.; Saigusa, Y.; Itoh, M. *J. Am. Chem. Soc.* **1991**, *113*, 4974−4980.
(58) Cozens, F. L.; Ortiz, W.; Schepp, N. P. *J. Am. Chem. Soc.* **1998**, *120*, 13543−13544.
(59) Andre, J. J.; Weill, G. *Mol. Phys.* **1968**, *15*, 97−99.
(60) Kawai, K.; Shirota, Y.; Tsubomura, H.; Mikawa, H. *Bull. Chem. Soc. Jpn.* **1972**, *45*, 77−81.
(61) Kemp, D. R.; Porter, G. *Chem. Commun.* **1969**, 1029−1030.
(62) The initial reflectance change did not remain completely constant at the different time scales. No corrections were made to account for these small differences, and this is reflected in the noise observed in the traces in Figure 2.
(63) Wagner, B. D.; Ware, W. R. *J. Phys. Chem.* **1990**, *94*, 3489−3494.

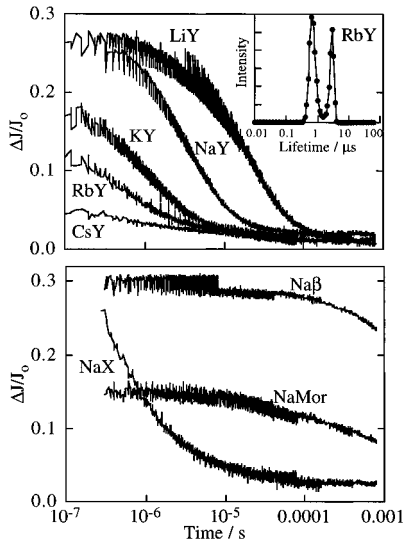

Figure 2. Top: Decay at 360 nm for the 4-methoxycumyl cation generated upon 266-nm excitation of 4,4′-dimethoxybicumene in the alkali metal cation-exchanged Y zeolites. The insert shows the lifetime distribution from the decay of the 4-methoxycumyl cation in RbY. Bottom: Decay at 360 nm for the 4-methoxycumyl cation generated upon 266-nm excitation of 4,4′-dimethoxybicumene in NaX, NaMor, and Naβ.

Table 2. Lifetime(s) of the 4-Methoxycumyl Cation in Various Alkali Cation Zeolites

zeolite	lifetimes[a]/μs	Si/Al	charge on oxygen[b]
LiY	26 (81%), 5.0 (19%)	2.4	−0.350
NaY	4.6 (100%)	2.4	−0.358
KY	1.0 (74%), 4.5 (26%)	2.4	−0.375
RbY	0.9 (58%), 0.3 (42%)	2.4	−0.378
CsY	0.4 (100%)	2.4	−0.391
NaX	0.5 (100%)	1.2	−0.413
NaMor	≈1000	6.5	−0.278
Naβ	≈3000	18	−0.240

[a] Lifetimes were calculated using the exponential series method or by fitting the data to single or double first-order rate equations. The values in the brackets refer to the fraction of the transient that decays with the corresponding lifetime. [b] Calculated using Sanderson electronegativity and the Sanderson equalization principle.

lifetimes of 26 and 5 μs. The major decay component making up 81% of the overall decay had the longer 26 μs lifetime, while the minor component at 19% had a 5 μs lifetime. The carbocation in NaY was significantly shorter-lived and decayed in a single-exponential fashion with a lifetime of 4.6 μs. In KY and RbY, the carbocation decays fit best to double first-order exponential equations. The shorter lifetime of 1 μs made up the majority, 74%, of the decay in KY, while in RbY a shorter lifetime of 0.3 μs contributed about 58% of the overall decay and the slightly longer lifetime component of 0.9 μs made up 42%. The weak decay in CsY fit to a single exponential with a lifetime of just 0.4 μs. These results are summarized in Table 2, and overall show a clear trend in which the lifetime of the 4-methoxycumyl cation decreases substantially upon going from LiY to CsY.

In NaX, only one component with a lifetime of 0.5 μs was observed for the decay of the 4-methoxycumyl cation. In both NaMor and Naβ, little decay was observed, Figure 2, over 1 ms, the longest time scale of the laser system, indicating that the carbocation is very long-lived in these zeolites. To obtain a rough estimate of the lifetime within these two zeolites, the small decay was fit to a first-order expression with the assumption that the carbocation decays completely to the baseline. Long lifetimes of ≈1000 μs in NaMor and ≈3000 μs in Naβ were obtained in this way.

Table 3. Kinetic Isotope Effects for the Decay of the 4-Methoxycumyl Cation in Alkali Cation Zeolites

zeolite	k_H/k_D
LiY	1.46 ± 0.20
NaY	1.30 ± 0.18
KY	1.40 ± 0.20
RbY	1.43 ± 0.20
CsY	1.39 ± 0.20

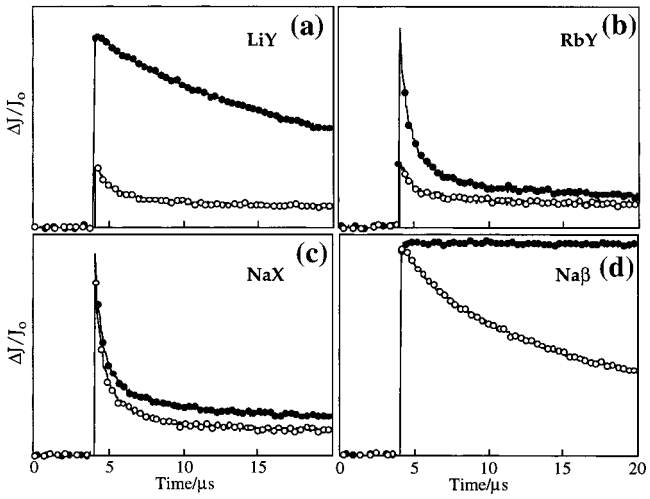

Figure 3. Decay at 360 nm for the 4-methoxycumyl cation generated upon 266-nm excitation of 4,4′-dimethoxybicumene in dry (closed circles) and hydrated (open circles) (a) LiY, (b) RbY, (c) NaX, and (d) Naβ.

Kinetic Isotope Effects on the Absolute Reactivity of the 4-Methoxycumyl Cation in Y Zeolites. Laser irradiation of 4,4′-dimethoxybicumene-d_{12} in each of the five alkali metal-exchanged Y-zeolites yields transient diffuse reflectance spectra showing the presence of two transients with maxima at 290 and 360 nm that are identical with those observed for the nondeuterated analogue in each alkali metal Y zeolite under both vacuum and oxygen conditions. The two transients can therefore be readily identified as the deuterated 4-methoxycumyl cation and 4-methoxycumyl radical.

The decay traces for the deuterated 4-methoxycumyl cation in the five alkali metal-exchanged zeolites are closely similar to the decay traces for the nondeuterated analogue in the same zeolites.[56] Kinetics for the d_6-carbocation were calculated in the same way as described previously for the h_6-carbocation, and the isotope effects shown in Table 3 were calculated from the ratio of the two rate constants, k_H/k_D. In each case, the observed rate constants for the decay of the 4-methoxycumyl-d_6 cation are only slightly slower than the corresponding nondeuterated carbocation with kinetic isotope effects, $k_H/k_D = 1.4 \pm 0.2$.

Effect of Water on Reactivity of the 4-Methoxycumyl Cation. As indicated by the weak absorption at 360 nm, Figure 3a,b, little or no 4-methoxycumyl cation is detectable after laser irradiation of 4,4′-dimethoxybicumene when water is co-incorporated into the cation-exchanged Y zeolites. This is consistent with the lifetime of the 4-methoxycumyl cation being reduced in the presence of water to the point where the carbocation can no longer be resolved with our laser system. The short lifetime can readily be explained by a quenching process that involves nucleophilic addition of a water molecule already present within the cavity in which the carbocation is born. Such an intracavity reaction, typically called a static

quenching process, is expected to be rapid since no diffusion of the two reacting species is required.

We also considered the possibilities that water inhibits the formation of the carbocation by rapidly quenching the 4,4′-dimethoxybicumene radical cation prior to C−C bond cleavage, or by interfering with the photoionization step. These possibilities were explored by examining the behavior of the 4-methoxytoluene radical cation generated by laser-induced photoionization of 4-methoxytoluene incorporated within the zeolite cavities. Our results show that the yield of the 4-methoxytoluene radical cation is unaffected by the presence of water or methanol within the zeolite cavities.[56] In addition, the 4-methoxytoluene radical cation is not quenched at all in the presence of co-incorporated nucleophiles and continues to have a very long lifetime of ∼10 μs within the zeolite cavities even when the water or methanol content is high with greater than 2 molecules of methanol per supercage. These results clearly suggest that the low yield of carbocation derived from 4,4′-dimethoxybicumene in the presence of water cannot be due to reduced efficiency of photoionization, or to rapid quenching of the 4,4′-dimethoxybicumene radical cation prior to C−C bond cleavage.

Static quenching of the 4-methoxycumyl cation by hydration also occurred in NaMor, but quite different results were observed in Naβ and NaX (Figure 3c,d). In Naβ, the addition of water had no effect on the initial signal of the 4-methoxycumyl cation indicating that no static quenching is taking place within this zeolite. However, the lifetime of the carbocation was significantly reduced by more than 2 orders of magnitude from ≈3000 μs to 25 μs. The effect of water in Naβ therefore exemplifies a dynamic quenching process that requires diffusion together of water and carbocation for the nucleophilic addition reaction to occur. In NaX, hydration had little effect on the initial absorption after the laser pulse and also had little effect on the lifetime of the carbocation which decreased slightly from 0.5 μs under dry conditions to 0.4 μs under hydrated conditions.

Intrazeolite Addition of Methanol to the 4-Methoxycumyl Cation. The addition of methanol to LiY, NaY, KY, RbY, and CsY had distinct effects on the behavior of the 4-methoxycumyl cation. First, in each of the zeolites except CsY, the rate constant for the decay of the carbocation increased with increasing amounts of methanol. This behavior indicates the presence of a dynamic quenching process whereby a methanol molecule in a remote cavity first diffuses over a time scale of several microseconds into the cavity containing the carbocation. Once the two reacting species are confined within the same cavity, an encounter complex is rapidly formed and then immediately collapses to quench the carbocation. Except in CsY where no dynamic quenching was observed, plots of the rate constant as a function of methanol content were all linear (Figure 4a). Linear least-squares analysis gave the second-order rate constants summarized in Table 4. The rate constants are all very similar, ranging from 2.0×10^5 M^{-1} s^{-1} in LiY to 5.9×10^5 M^{-1} s^{-1} in RbY.

In addition to the dynamic quenching, the initial intensity of the reflectance change immediately after the laser pulse at 360 nm due to absorption by the carbocation decreases significantly in the presence of methanol. This was observed in all of the cation-exchanged zeolites, including CsY. Since, as described earlier, the yield and lifetime of the radical cation are not influenced by methanol, the decrease represents a static quenching process whereby some of the carbocations are rapidly quenched by methanol in an intracavity reaction. As shown in Figure 4b, the magnitude of the static quenching increases as a function of methanol content. A linear relationship is observed, with the slopes changing slightly upon going from LiY to CsY.

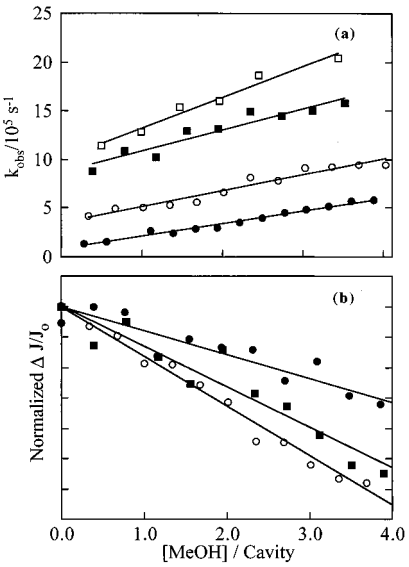

Figure 4. Relationship between (a) the observed rate constant for decay and (b) the initial absorption at 360 nm for the 4-methoxycumyl cation and the concentration of methanol in LiY (closed circles), NaY (open circles), KY (closed squares), and RbY (open squares).

Table 4. Quenching Rate Constants for the Reaction of the 4-Methoxycumyl Cation with Methanol in Alkali Metal Cation-Exchanged Zeolites

zeolite	rate constant/M^{-1} s^{-1}	rel quenching constant
LiY	$(2.0 \pm 0.2) \times 10^5$	0.7
NaY	$(2.7 \pm 0.3) \times 10^5$	1
KY	$(3.8 \pm 0.4) \times 10^5$	1.4
RbY	$(5.9 \pm 0.6) \times 10^5$	2.2
CsY	no quenching	no quenching

Table 5. Relative Quenching Rate Constants for the Reaction of the 4-Methoxycumyl Cation with Simple Alcohols in NaY

alcohol	rel quenching constant
methanol	1
ethanol	0.51
2-propanol	0.31
1-butanol	0.25
2-methyl-2-propanol	0.19
tert-butyl alcohol	no quenching

In Naβ, the rate constant for the decay of the carbocation increased dramatically upon the addition of small amounts of methanol indicating the presence of dynamic quenching, while no static quenching was observed. The opposite result was obtained for NaMor, where static quenching by methanol was seen, but dynamic quenching was not. In NaX no quenching of the carbocation by methanol, either dynamic or static, was observed.

Addition of Other Alcohols to the 4-Methoxycumyl Cation in NaY. Similar results to those described above for the addition of methanol to the 4-methoxycumyl cation in NaY were observed upon quenching of the carbocation with ethanol and 2-propanol. However, in both cases, dynamic quenching is considerably reduced relative to methanol. As shown in Table 5, quenching rate constants for ethanol and 2-propanol are about 2-fold and 3-fold, respectively, slower than that for methanol. Dynamic quenching of the 4-methoxycumyl cation by either 1-butanol or 2-butanol was even less effective and reacted with rate constants about 4-fold and 5-fold, respectively, slower than

methanol, indicating that the efficiency of dynamic quenching decreases with increasing chain branching. In the presence of *tert*-butyl alcohol, no dynamic quenching was observed as the carbocation lifetime was found to be independent of alcohol concentration.

While the size of the alcohol seems to have a significant effect on the dynamic quenching rate constants, the magnitude of the static quenching remains relatively unaffected. Even though there is some scatter in the static quenching data[56] it is evident that the decrease in the intensity of the carbocation signal at 360 nm in the presence of the larger alcohols such as *tert*-butyl alcohol is very similar to that observed for the smaller alcohols such as methanol, Figure 4b, and ethanol in NaY.

Product Studies. Steady-state irradiation of 4,4′-dimethoxybicumene under a continuous flow of dry nitrogen or argon in NaY for ~80 h followed by addition of methanol to the zeolite composite and extraction with dichloromethane gave the five compounds shown in eq 3. The products, which were identified

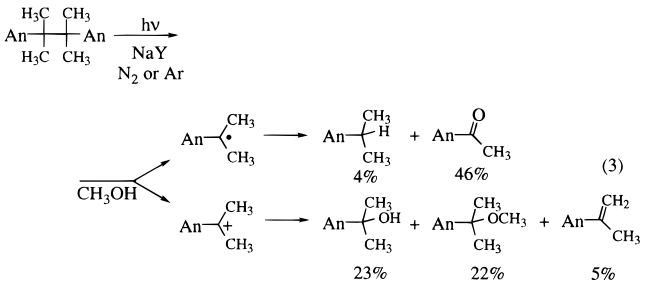

(3)

and quantified by a combination of GC, GC/MS, and HPLC, are derived from the 4-methoxycumyl radical and the 4-methoxycumyl cation in a 1:1 ratio and are consistent with the rapid fragmentation of the photogenerated 4,4′-dimethoxybicumene radical cation as observed by laser studies within zeolites and as previously measured for the radical cation in solution.[52,53]

4-Methoxycumyl alcohol and 4-methoxycumyl methyl ether together account for 90% of the carbocation-derived products.[64] As methanol was only added to the zeolite sample *after* the photolysis was complete, formation of the ether cannot be attributed to direct attack of methanol on the free carbocation. It must instead be produced via reaction of an initial carbocation−nucleophile adduct, such as a long-lived framework-bound alkoxy species (vide infra). A similar mechanism also can account for the formation of the alcohol since water is adsorbed by the zeolite composite following the photolysis and during the extraction. However, although great care was taken to conduct the photolysis under anhydrous conditions, the possibility that a small amount of water adsorbed during the lengthy photolysis period trapped some of the free carbocation cannot be ruled out. Interestingly, deprotonation of the 4-methoxycumyl cation to give α-methyl-4-methoxystyrene is a minor pathway, accounting for only 10% of the carbocation-derived products.

The most abundant radical photoproduct was 4-methoxyacetophenone (46%). Additional experiments were conducted to establish that this product originates from oxygen-trapping of the 4-methoxycumyl radical. First, acetophenone was produced as a major photoproduct (ca. 50%) upon formation of the cumyl radical by selective irradiation of di-*tert*-butyl peroxide within NaY in the presence of cumene under a continuous flow of nitrogen. Observation of significant ketone formation under these conditions indicates that the concentration of oxygen within the zeolite framework is sufficient to trap this radical even under a continuous flow of nitrogen. In addition, to rule out the possibility that the ketone was produced by secondary photolysis of α-methyl-4-methoxystyrene, this olefin was irradiated in NaY under a continuous flow of dry nitrogen. No detectable amounts of 4-methoxyacetophenone were observed for conversions as high as 35%, suggesting that the concentration of oxygen within the zeolite framework in nitrogen-saturated NaY is insufficient to lead to competitive olefin oxidation.

Discussion

Mechanism for Intrazeolite Decay of the 4-Methoxycumyl Cation. Our results demonstrate unambiguously that the 4-methoxycumyl cation has a lifetime in the microsecond to millisecond range in dry alkali metal cation-exchanged zeolites, even under conditions where coadsorbed nucleophiles are excluded. These relatively short lifetimes can therefore be attributed to a direct interaction between the carbocation and the zeolite host in which it is encapsulated. In a manner analogous to the reactions of carbocations in solution, the mechanism for this intrazeolite decay can be envisioned as taking place via nucleophilic addition or deprotonation pathways. For instance, the zeolite framework may act as a nucleophile adding to the carbocation to generate a zeolite−carbocation adduct. Alternatively, the zeolite may act as a base, deprotonating the carbocation to give the corresponding styrene.

Steady-state irradiation of 4,4′-dimethoxybicumene in NaY clearly demonstrates that the major carbocation-derived products obtained can be accounted for by nucleophilic addition (90%), rather than deprotonation (10%). The role of the zeolite as a base toward carbocation deprotonation is therefore a minor pathway. The kinetic isotope effects are also consistent with deprotonation playing only a minor role in the decay pathway of the carbocation within zeolites. Deprotonation of cumyl cations in solution using various bases typically shows a kinetic isotope effect in the range of $k_H/k_D \approx 4-5$.[65,66] The measured kinetic isotope effects of $k_H/k_D = 1.4 \pm 0.2$ in all of the cation-exchanged zeolites are close to unity. These values are considerably less than that expected for a reaction in which the zeolite acts as a base to remove a proton from the carbocation, and are more consistent with values expected for a mechanism that is dominated by nucleophilic addition.[65−67] Furthermore, the similarity of the isotope effects in each of the zeolites examined indicates that the mechanism is consistently nucleophilic addition and that the decreased lifetime as the zeolite counterion size is increased cannot be due to enhanced rate constants for deprotonation.

The 4-methoxycumyl alcohol and 4-methoxycumyl methyl ether produced under steady-state photolysis conditions arise from the addition of water and methanol, respectively. Since the majority of the 4-methoxycumyl cations live only about ~5 μs in NaY and methanol was added to the photolysis mixture after irradiation, the generation of 4-methoxycumyl methyl ether

(64) As suggested by a referee, we considered the possibility the alcohol and ether were derived from the α-methyl-4-methoxystyrene during the workup, especially since a small amount of protons would be generated upon formation of the styrene. To test for this possibility, the styrene was incorporated in NaY containing added protons and methanol, and then extracted in the same manner as in the product studies. No methyl ether was formed, and only a small amount (<0.01%) of alcohol was produced. These results indicate that the styrene is not converted to a significant extent to the carbocation derived products under our reaction conditions.

(65) Thibblin, A. *J. Phys. Org. Chem.* **1989**, *2*, 15−25.

(66) Thibblin, A. *Chem. Soc. Rev.* **1993**, *22*, 427−433.

(67) The isotope effect for nucleophilic substitution should in principle be closer to unity than that measured in the present work, and may even be slightly less than one. Our measured value of $k_H/k_D = 1.4 \pm 0.2$ may therefore include a component for deprotonation which, based on product studies, accounts for about 10% of the decay of the carbocation and should show a substantial normal isotope effect.

cannot be attributed to nucleophilic trapping of the initially formed free carbocation. Instead, the carbocation must decay to some metastable product which subsequently reacts with methanol to give the observed product. A reasonable mechanism for carbocation decay, then, involves nucleophilic attack of the zeolite framework on the free carbocation leading to the formation of a framework-bound alkoxy species, eq 4. The methyl ether is then formed by a solvolysis type reaction of the alkoxy species upon the introduction of methanol.[68−71]

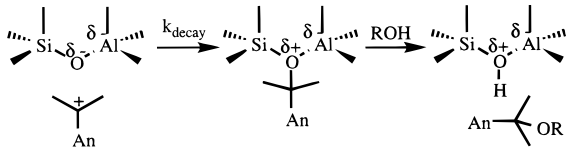

(4)

The alcohol can also be produced through the same reaction pathway, with water being adsorbed by the zeolite after photolysis is complete. We cannot rule out the possibility that a sufficient amount of water was adsorbed by the zeolite during photolysis to trap the free carbocation directly and account for all alcohol formation. However, our precautions in keeping the zeolite dry prior to and during photolysis make this possibility unlikely.

There is considerable evidence from infrared[72,73] and solid-state NMR studies of carbocations in Brønsted acid zeolites[40,68−71,74−76] and a variety of uni- and divalent metal exchanged zeolites[77−80] for the existence of framework-bound alkoxy species. Within protic zeolites, such framework-bound alkoxy species have been proposed as mechanistic alternatives to long-lived free carbocations which achieve considerable stabilization through covalent attachment to nucleophilic framework sites.[40,81] Thus with the exception of a few highly stabilized carbocations that exist as persistent free species within Brønsted acid zeolites, carbocations are trapped by the nucleophilic lattice oxygens, either concurrent with carbocation formation (i.e. in an S_N2-like process) or after some finite lifetime as a transient intermediate (i.e. an S_N1-like process). Similar types of reaction dynamics have been proposed to occur within nonprotic zeolites. For instance, the conversion of methyl iodide to ethylene within metal ion zeolites has been described as "acid−base bifunctional catalysis"[77,78] that can be formally envisioned as an S_N2-like process whereby the zeolite framework acts as a nucleophile while the metal cation promotes loss of the leaving group. The emerging picture is a continuum of intermediates,[40] from free carbocations stabilized by intermolecular interactions and the electrostatic fields within the zeolite, to covalently bound intermediates deriving stabilization from the attachment to electron rich framework sites. Ultimately the transition from one extreme to the other will depend on the inherent stability of the carbocation within the zeolite microenvironment, and on the nucleophilicity exerted by the zeolite framework.

Reactivity of the 4-Methoxycumyl Cation in Dry Zeolites: Zeolite Nucleophilicity. The lifetimes of the 4-methoxycumyl cation in the various zeolites examined in the present work are summarized in Table 2. The lifetimes span a remarkably wide range, with the carbocation having a lifetime that is almost 10000-fold longer in Naβ than in CsY! These results therefore provide dramatic evidence that carbocation lifetime within nonacid zeolites can be effectively controlled by changing the counterion, Si/Al ratio, and morphology of the zeolite.

One trend that is evident from the data in Table 2 is that the lifetime decreases in a systematic manner as the cation is varied from Li^+ to Cs^+. This trend clearly illustrates that the charge-balancing cation must play an important role in regulating the kinetic behavior of carbocations embedded within Y zeolites. The mechanism by which the cation exerts its influence on the carbocation reaction can be related to the effect of cation-exchange in Y zeolites on the Lewis basicity of the [Si−O−Al] active sites within the framework, an effect that has recently been emphasized in several studies.[16,27,82,83] In particular, the Cs^+-exchanged Y zeolite is a considerably stronger Lewis base than the Li^+-exchanged Y zeolite by virtue of the weak interaction between the large diffuse Cs^+ cation and the negative charge at the [Si−O−Al] active site. This increased Lewis basicity as the counterion is changed from Li^+ to Cs^+ is manifested as a significant increase in nucleophilicity of the framework oxygens and gives rise to the large 65-fold decrease in lifetime of the carbocation.

In addition to being affected by the counterion, the kinetic behavior of the 4-methoxycumyl cation is strongly influenced by the Si/Al ratio. For example, the lifetime decreases considerably by a factor of 9 upon going from NaY, which has a Si/Al = 2.4, to NaX, with a Si/Al = 1.2. This is consistent with the notion that the framework participates directly in the quenching of the carbocation by nucleophilic addition. In fact, numerous studies have shown that the basicity in zeolites does increase as the Si/Al ratio decreases.[10,16,27,82−88] An increase in Lewis base strength of the zeolite would result in an increase in the nucleophilicity of the active sites which correlates nicely with the increase in the reactivity of the 4-methoxycumyl cation in NaX as compared to NaY. It must also be recognized that the number of Si−O−Al bridges within the supercages of NaX is greater than that in NaY. NMR studies have shown that framework-bound carbocations covalently attach to the oxygen atoms of Si−O−Al bridges, and theoretical studies have shown that the oxygen atoms of Si−O−Al bridges bind carbocations significantly more strongly than the oxygen atoms of Si−O−

(68) Haw, J. F.; Richardson, B. R.; Oshiro, I. S.; Lazo, N. D.; Speed, J. A. *J. Am. Chem. Soc.* **1989**, *111*, 2052−2058.
(69) Lazo, N. D.; White, J. L.; Munson, E. J.; M., L.; Haw, J. F. *J. Am. Chem. Soc.* **1990**, *112*, 4050−4052.
(70) Aronson, M. T.; Gorte, R. J.; Farneth, W. E.; White, D. *J. Am. Chem. Soc.* **1989**, *111*, 840−846.
(71) Bronnimann, C. E.; Maciel, G. E. *J. Am. Chem. Soc.* **1986**, *108*, 7154−7159.
(72) Forester, T. R.; Howe, R. F. *J. Am. Chem. Soc.* **1987**, *109*, 5076−5082.
(73) Ono, Y.; Mori, T. *J. Chem. Soc., Faraday Trans. 1* **1981**, *77*, 2209−2221.
(74) Oliver, F. G.; Munson, E. J.; Haw, J. F. *J. Phys. Chem.* **1992**, *96*, 8106−8111.
(75) Stepanov, A. G.; Zamaraev, K. I.; Thomas, J. M. *Catal. Lett.* **1992**, *13*, 407−422.
(76) Tsiao, C.; Corbin, D. R.; Dybowski, C. *J. Am. Chem. Soc.* **1990**, *112*, 7140−7144.
(77) Murray, D. K.; Howard, T.; Goguen, P. W.; Krawietz, T. R.; Haw, J. F. *J. Am. Chem. Soc.* **1994**, *116*, 6354−6360.
(78) Murray, D. K.; Chang, J.; Haw, J. F. *J. Am. Chem. Soc.* **1993**, *115*, 4732−4741.
(79) Bosacek, V. *Z. Phys. Chem.* **1995**, *189*, 241−250.
(80) Bosacek, V. *J. Phys. Chem.* **1993**, *97*, 10732−10737.
(81) Xu, T. *J. Am. Chem. Soc.* **1994**, *116*, 10188−10195.
(82) Lavalley, J.; Lamotte, J.; Travert, A.; Czyzniewska, J.; Ziolek, M. *J. Chem. Soc., Faraday Trans. 1* **1998**, *94*, 331−335.
(83) Choi, S. Y.; Park, Y. S.; Hong, S. B.; Yoon, K. B. *J. Am. Chem. Soc.* **1996**, *118*, 9377−9386.
(84) Barthomeuf, D. *J. Phys. Chem.* **1984**, *88*, 42−45.
(85) Haung, M.; Adnot, A.; Kaliaguine, S. *J. Catal.* **1992**, *137*, 322−332.
(86) Okamoto, Y.; Ogawa, M.; Maezawa, A.; Imanaka, T. *J. Catal.* **1988**, *112*, 427−436.
(87) Weirzchowski, P. T.; Zatorski, L. W. *Catal. Lett.* **1991**, *9*, 411.
(88) Corma, A.; Fornés, V.; Martín-Aranda, R. M.; García, H.; Primo, J. *Appl. Catal.* **1990**, *59*, 237−248.

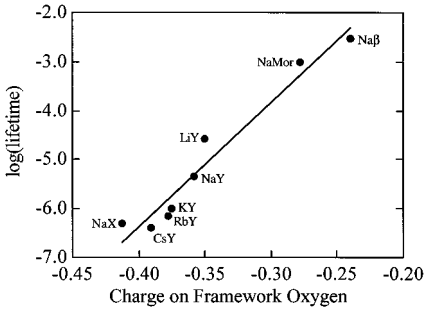

Figure 5. Relationship between lifetime of the 4-methoxycumyl cation and charge on framework oxygen.

Si bridges.[89,90] As a result, the Si−O−Al sites are considerably more nucleophilic, and the smaller Si/Al ratio in NaX translates into an increase in the number of potential nucleophilic sites which presumably contributes to the higher reactivity of the carbocation in NaX compared to NaY.

The 4-methoxycumyl cation is quite long-lived in NaMor and Naβ, with estimated lifetimes of ca. 1000 and 3000 μs, respectively. These zeolites have high Si/Al ratios (NaMor, Si/Al = 6.5 and Naβ, Si/Al = 18) which suggests that the lower reactivity of the carbocation is due to a combination of reduced nucleophilicity at each active site and a large overall reduction in the number of nucleophilic Si−O−Al sites relative to the nonnucleophilic Si−O−Si sites. Another important factor that must be considered, especially with respect to NaMor, is the rigorous confinement of the carbocation within the channel-like morphology (Table 1). This tight molecular confinement may make it more difficult for the carbocation to locate an active site and to adopt an orientation that satisfies the electronic and steric requirements necessary to form the framework-bound alkoxy species.

Since nucleophilicity is an important parameter that determines the lifetime of the carbocations within these solid supports, the observed lifetime trend should follow the magnitude of the partial negative charge associated with the oxygen atoms in the framework. Sanderson concepts of electronegativity and charge density at the lattice oxygen atoms have previously been applied to zeolites,[84,91−93] and more recently have been used to describe basicity in alkali metal zeolites.[27,83] Partial charges on oxygen can be calculated using the Sanderson equalization principle.[94−97] These values are given in Table 2 for all of the zeolites examined in the present work. A plot of the carbocation lifetime as a function of the charge on the framework oxygen is shown in Figure 5. When all of the zeolites examined in the present work are included, a clear trend is observed in which the lifetime increases as the charge on the oxygen decreases, which is consistent with a decrease in overall nucleophilicity of the zeolite. Interestingly, an analogous trend has been recently observed in a study that correlated the observed ^{13}C chemical shifts of framework-bound methoxy groups to the Sanderson electronegativity of a series of nonprotic zeolite frameworks.[79,80] The chemical shift trend was explained in terms of zeolite nucleophilicity and the formation of the framework-bound methoxy groups was attributed to direct nucleophilic attack on the electrophilic guest molecule.

The ability of the various zeolites to stabilize the incorporated carbocation must also be considered. The electrostatic fields within the zeolite cavities are typically assumed to play an important role in stabilizing charged organic compounds such as carbocations. The strength of these fields depends on the size of the counterion and decreases as the size of the counterion increases.[98] Thus, the observed decrease in the lifetime upon going from LiY to CsY may, in part, reflect a decrease in the inherent ability of the zeolites to support the presence of the positively charged carbocation. On the other hand, for a given counterion, the electrostatic field, and thus the stabilizing ability of the zeolites, decreases as the Si/Al ratio increases. Thus, based on electric field strength alone, the lifetime of the carbocation should decrease as the Si/Al ratio increases. This is opposite from that observed in the present work for NaX, NaY, NaMor, and Naβ, and supports the notion that weaker nucleophilicity and fewer nucleophilic sites as the Si/Al ratio increases play the dominant role in determining the lifetime of the carbocation.

Nucleophilic Addition Reactions of Alcohols to the 4-Methoxycumyl Cation. In the presence of coadsorbed methanol in NaY the 4-methoxycumyl cation is quenched by two distinct processes. Dynamic quenching is observed where the rate constant for the disappearance of the 4-methoxycumyl cation increases linearly with increasing concentration of methanol. Rapid static quenching ($>10^8$ s^{-1}) is also observed, such that the amount of carbocation remaining after the 10 ns laser pulse decreases with increasing methanol content. Observing static quenching is significant because it suggests that a rapid reaction takes place when the alcohol and the carbocation are confined within the same cavity. As a result, it is reasonable to conclude that dynamic quenching represents a process in which the alcohol diffuses slowly into the cavity containing the carbocation (Scheme 1, step a) and then undergoes a rapid intracavity addition reaction (Scheme 1, step b), while static quenching involves only the rapid intracavity reaction (Scheme 1, step b). This contrasts sharply with the behavior observed in solution. For instance, methanol quenching of the 4-methoxycumyl cation in 2,2,2-trifluoroethanol (TFE) is activation controlled with typical bimolecular rate constants of ca. 5×10^6 M^{-1} s^{-1},[99] which are much smaller than the diffusional limit. Thus, the encounter complex between the alcohol and the carbocation proceeds more readily to product within the zeolite matrix than in solution, and the zeolite actually *enhances* the reactivity of the nucleophile toward static quenching of the carbocation. The role of the zeolite may be largely *passive*, with the enhanced reactivity being derived from the entropic effects associated with molecular confinement. However, it is quite conceivable that the zeolite is an *active* participant, whereby the electron-rich lattice oxygens promote nucleophilic addition by enhancing the deprotonation of the nucleophile as it attacks the carbocation, or by assisting the deprotonation of the resultant oxonium ion adduct.

Despite the rapid intracavity reaction of the alcohol and the carbocation, the second-order rate constants for the bimolecular reactions between the alcohol and the carbocation are quite small. This is certainly associated with the heterogeneous topology of the framework, which hinders the mobility of the

(89) Kramer, G. J.; van Santen, R. A. *J. Am. Chem. Soc.* **1993**, *115*, 2887−2897.
(90) Mota, C. J. A.; Esteves, P. M.; de Amorim, M. B. *J. Phys. Chem.* **1996**, *100*, 12418−12423.
(91) Jacobs, P. A.; Mortier, W. J.; Uytterhoeven, J. B. *J. Inorg. Nucl. Chem.* **1978**, *40*, 1919−1923.
(92) Mortier, W. *J. Catal.* **1978**, *55*, 138−145.
(93) Mortier, W.; Schoonheydt, R. A. *Prog. Solid State Chem.* **1985**, *16*, 1−125.
(94) Sanderson, R. T. *Chemical Bonds and Bond Energy*, 2nd ed.; Academic Press: New York, 1976.
(95) Sanderson, R. T. *J. Am. Chem. Soc.* **1983**, *105*, 2259−2261.
(96) Sanderson, R. T. *J. Chem. Educ.* **1988**, *65*, 112−118.
(97) Sanderson, R. T. *J. Chem. Educ.* **1988**, *65*, 227−231.
(98) Ward, J. W. *J. Catal.* **1968**, *10*, 34−46.
(99) Cozens, F. L. Ph.D. Thesis, University of Toronto, 1992.

Scheme 1

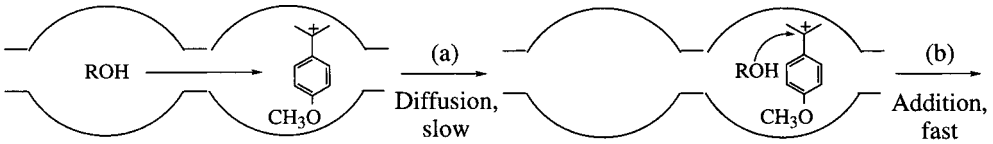

quencher as it diffuses through the channels and cavities of the zeolite. As such it exemplifies the capacity of zeolitic media to influence bimolecular reactions of incorporated reagents in a passive sense.

The importance of hindered diffusion is also evident when comparing the effect of alcohol structure on the rate constants for quenching of the 4-methoxycumyl cation in NaY. From the data summarized in Table 5, it is evident that dynamic quenching decreases by a factor of 5 as the size of the alcohol increases from methanol to 2-methyl-1-propanol, and that no dynamic quenching at all is observed with the bulky *tert*-butyl alcohol. At the same time, static quenching is not significantly affected, indicating that the actual nucleophilic addition step within the cavity remains rapid even as the steric bulk of the alcohol is considerably increased. Thus, the large decrease in the dynamic quenching of the 4-methoxycumyl cation within the NaY zeolite reflects a slower diffusion of the large alcohols through the framework to a cavity containing the carbocation.

The observation that the rate constants for dynamic quenching increase as the counterion becomes larger upon going from Li^+ to Rb^+ suggests that the rate of diffusion of methanol increases as the size of the counterion increases. This is not consistent with a simple steric model for diffusion of alcohols within the open framework of the zeolite that would result in a decrease in the rate of diffusion as the counterion becomes larger. However, other factors are also important in defining the mobility of alcohols. In particular, recent studies have shown that the electrostatic interaction between hydroxyl-containing molecules and intrazeolite cations decreases considerably as the size of the cations increases. For example, temperature-desorption studies have shown that water molecules in Li^+-containing zeolites require up to 20 kJ/mol more energy for desorption than water molecules from zeolites containing large cations such as Rb^+.[100,101] As a result, inhibition of alcohol migration due to electrostatic interactions will decrease as the cation becomes larger, causing an increase in the diffusion of the methanol molecules and a slight increase in the rate of the dynamic quenching. In the case of CsY where no dynamic quenching is observed, it is likely that unfavorable steric factors dominate over the electrostatic binding, with the Cs^+ counterion being sufficiently large to effectively block the mobility of methanol. Thus, diffusion of methanol around the large Cs^+ cations into cavities containing the carbocation is too slow to compete with the very fast intracavity trapping of the carbocation by nucleophilic addition to the CsY framework.

Similar arguments can be used to provide an explanation for the absence of dynamic quenching in NaX. NaX contains a significantly greater number of sodium ions than NaY. Since methanol coordinates strongly to the metal cations, the efficiency of migration is significantly reduced in NaX,[102,103] and the magnitude of dynamic quenching in NaX is less than that observed in NaY. In addition, the 4-methoxycumyl cation reacts quite rapidly with the NaX framework. As a result, even if dynamic methanol quenching in NaX was comparable to that observed in NaY, the decrease in the lifetime of the carbocation in NaX would be marginal and difficult to observe.

Unlike the situation in NaY where both dynamic and static quenching were observed upon addition of methanol, only dynamic quenching of the 4-methoxycumyl cation was observed in Naβ. One possible explanation for the absence of static quenching is that the carbocation is generated at a site within the framework that is remote from any sites containing methanol. While this situation might exist in Naβ due to its high Si/Al ratio, the relatively large amount of methanol used in these studies (up to 10 wt %) renders this explanation unlikely. Alternatively, as suggested above, basic sites of the zeolite framework might play a role in facilitating the nucleophilic addition of methanol to the carbocation. Since the number of such sites and the basicity of each site is low in Naβ, the ability of Naβ to aid in the actual nucleophilic addition step is considerably reduced compared to NaY, and rapid static quenching is not observed. This is consistent with the fact that the quenching rate constant in Naβ is 130-fold smaller than that in NaY.[104] Thus, since the encounter complex in Naβ does not rapidly collapse to quench the carbocation, dynamic quenching is not diffusion limited, but instead becomes activation controlled. In NaMor, dynamic quenching was not observed. In this case, the mobility of the methanol is presumably inhibited by the 1-dimensional morphology of the zeolite.

Reactivity of the 4-Methoxycumyl Cation in Zeolites: Influence of Hydration. In the Y zeolites, the addition of water (2−12 wt %) to the 4,4′-dimethoxybicumene/zeolite composites prior to laser irradiation quenches almost all of the photogenerated 4-methoxycumyl cations during the laser pulse, and the lifetime of the carbocations under these conditions can therefore be estimated to be <20 ns. Since the lifetime in the presence of water is considerably less than that in the absence of water, the dominant mode of decay of the carbocation upon hydration is nucleophilic addition of water. The short lifetime presumably reflects a significant degree of static quenching whereby the carbocations are trapped rapidly by water present within the same cavity in which the carbocation was initially generated. The effects of water on the lifetime of the carbocation in NaX, Naβ, and NaMor are essentially the same as those observed upon the addition of methanol. The explanation for these effects is therefore similar to that described above for methanol quenching. Thus, in NaX, the water molecules are rendered less nucleophilic due to the interactions with the large number of sodium cations. In Naβ, the small number of active sites reduces the ability of the framework to assist in the nucleophilic addition reaction, while the 1-dimensional morphology of NaMor restricts access of the water molecules to the reactive carbocation.

(100) Kirmse, A.; Karger, J.; Stallmach, F.; Hunger, B. *Appl. Catal. A* **1999**, *188*, 241−246.

(101) Hunger, B.; Klepel, O.; Kirchhock, C.; Heuchel, M.; Toufar, H.; Fuess, H. *Langmuir* **1999**, *15*, 5937−5941.

(102) Ramamurthy, V. *J. Am. Chem. Soc.* **1994**, *116*, 1345−1351.

(103) Karger, J.; Pfeifer, H. In *NMR Techniques in Catalysis*; Bell, A. T., Pines, A., Eds.; Marcel Dekker: New York, 1994; Chapter 2.

(104) The quenching rate constant in Naβ was measured to be 7.5×10^4 mg mol^{-1} s^{-1} which compares to a value of 1×10^7 mg mol^{-1} s^{-1} in NaY. These values were determined from the relationship between observed rate constants for the decay of the 4-methoxycumyl cation as a function of moles of methanol per mg of Naβ or NaY.

Conclusions

Rapid fragmentation of the photogenerated 4,4′-dimethoxybicumene radical cation is a convenient, efficient technique for the generation and study of the reactive 4-methoxycumyl cation in nonprotic zeolites. A likely mechanism for intrazeolite decay of the 4-methoxycumyl cations involves direct attack of electron rich lattice oxygens in the framework, and the carbocation lifetime is thus strongly dependent on the *zeolite nucleophilicity*. Such a mechanism is consistent with numerous studies in Brønsted acidic zeolites, where many carbocations have been shown to exist as framework-bound alkoxy species rather than free ions. As a result, the absolute lifetime of the carbocation within the zeolite matrix can be tuned by altering zeolite characteristics such as the charge-balancing cation, Si/Al ratio, and/or framework morphology which are directly correlated to the nucleophilicity of the framework. Similarly, bimolecular nucleophilic addition of alcohols and water to carbocations can be modulated by simple variations in the zeolite composition and morphology. This is again attributed to the fact that the zeolite is not simply a passive medium for encapsulating electrophilic reagents, but in fact exerts an active role in the uni- and bimolecular chemistry of carbocation guests.

Experimental.

Materials. 4,4′-Dimethoxybicumene was prepared by radical-initiated dimerization of 4-methoxycumene according to literature procedures[105] and purified by sublimation to yield a white solid (mp 173−175 °C). ^{1}H NMR (250 MHz, $CDCl_3$) δ 6.85 (dd, 8H), 3.85 (s, 6H), 1.3 (s, 12 H); ^{13}C NMR (62.5 MHz, $CDCl_3$) δ 25.3, 43.1, 55.2, 111.9, 129.6, 139.1, 157.3. 4,4′-Dimethoxybicumene-d_{12} was similarly prepared by dimerization of 4-methoxycumene-d_6 (1,1,1,3,3,3-hexadeuterio-2-(4-methoxyphenyl)propane) and purified by column chromatography (1% ethyl acetate in hexanes). Recrystallization from hexane−dichloromethane mixtures afforded a white crystalline solid (mp 173−175 °C). ^{1}H NMR (250 MHz, $CDCl_3$) δ 6.85 (dd, 8H), 3.85 (s, 6H); ^{13}C NMR (62.5 MHz, $CDCl_3$) 23.3 (septet), 42.6, 55.2, 111.9, 129.6, 139.1, 157.3. The deuterated precursor, 4-methoxycumene-d_6, was prepared by Grignard addition of acetone-d_6 to 4-bromoanisole and subsequent reduction of the corresponding alcohol using trifluoroacetic acid and sodium borohydride.[106] The alcohols, methanol, ethanol, 2-propanol, 2-methyl-1-propanol, 1-butanol, and *tert*-butyl alcohol, were of spectroscopic grade (Aldrich) and used as received.

NaY, Si/Al = 2.4, and NaX, Si/Al = 1.2, were obtained from Aldrich. Naβ, Si/Al = 18, and NaMordenite, Si/Al = 6.5, were obtained from the P.Q. Corporation. All zeolites were used as received after activation at 400 °C for 16 h to remove any co-incorporated water. The exchanged zeolites were prepared by stirring NaY with 1 M aqueous solutions of the corresponding chlorides (LiCl, KCl, RbCl, and CsCl) at 80 °C for 1 h. The zeolites were then washed until no chlorides appeared in the washing water and dried under vacuum. This procedure was repeated three times and the zeolite was calcinated between washings. NaY has three types of exchangeable cations. The number of cations per unit cell of zeolite Y are 16 site I cations, 32 site II cations, and 8 site III cations. It is well established that only site II and III cations are accessible to guest molecules.[2] The percent exchange is typically 47% for LiY, 97% for KY, 44% for RbY, and 47% for CsY. It is known that for the larger cations such as Rb^+ and Cs^+ only the accessible Na^+ which occupy type II and type III sites can be readily exchanged.[15] Thus, the maximum accessible cation exchange is ∼70%. Values of ∼50% exchange indicate that a small percentage of type II cations are not completely exchanged. The low percent exchange for the LiY sample used in this study is because hydrated Li^+ also does not readily exchange the type II cations.

Sample Preparation. 4,4′-Dimethoxybicumene was incorporated into NaY using hexanes as a carrier solvent. Samples for laser experiments were prepared such that the loading level was approximately one molecule in every 10 supercages. The typical procedure involved introducing ca. 1 mL of a stock solution of the organic compound to ca. 250 mg of activated zeolite in 20 mL of hexane. For steady-state irradiations and product studies, larger zeolite samples with slightly higher concentrations of the bicumene were used. Thus, 100−180 mg of compound was combined with 2−3 g of NaY resulting in loading levels of approximately one molecule in every 2−3 supercages. The hexane slurry was stirred for 1−3 h, after which time the suspension was centrifuged and the isolated zeolite washed using hexane and dried under vacuum, 10^{-3} Torr. UV analysis of the combined decants indicated that 100% of the organic precursor was incorporated within NaY. During the incorporation of the precursor into the zeolite framework the utmost care was taken to keep the zeolite sample dry. After vacuum-drying for several hours, the zeolite samples were transferred to laser cells in a nitrogen-filled glovebag and then reevacuated to 10^{-3} Torr for an additional 10−12 h before the photolysis experiments. Samples for steady-state irradiation were placed in photolysis cells under an atmosphere of nitrogen and purged with nitrogen or argon for at least 30 min prior to irradiation. A continuous flow of dry nitrogen or argon was maintained throughout the photolysis. Detailed weight analysis studies were carried out on several NaY and NaX samples to determine the percent weight water contained in the zeolite after sample preparation. The results indicate that after sample preparation as described for the diffuse reflectance laser studies, the zeolite samples typically contain little, if any, water, certainly less than 1 wt %.

The procedure for incorporation of 4,4′-dimethoxybicumene into the other cation-exchanged zeolites was essentially identical with that for incorporation into NaY. The initial amount of 4,4′-dimethoxybicumene was adjusted to account for the reduced percent incorporation in the larger alkali cation zeolites, such that the final concentration was one molecule in every 10 supercages for all faujasites examined. The co-incorporation of 4,4′-dimethoxybicumene and chloranil was accomplished by initially preparing a NaY sample containing chloranil using dichloromethane as the carrier solvent. The loading level was one chloranil per 10 zeolite cavities. After the sample was dried under vacuum, 4,4′-dimethoxybicumene was incorporated into the chloranil/zeolite composites in the same manner as described above.

Hydration Experiments. Zeolite samples were hydrated by exposing a known quantity of the vacuum-dried 4,4′-dimethoxybicumene/zeolite composite to the atmosphere. The sample was spread into a thin layer on a shallow dish to allow for efficient hydration. The changes in sample mass due to water uptake were monitored until no further change in mass was observed. The final concentration of water in the hydrated zeolite was dependent on the charge balancing cation, Si/Al ratio, and framework morphology. Typical values of water uptake (expressed as weight percent) by the 4,4′-dimethoxybicumene/zeolite composites are ca. 12%, 10%, 6%, 3%, and 2% for the alkali metal zeolites LiY through CsY, respectively, and ca. 5%, 4%, and 3% for NaX, NaMor, and Naβ, respectively.

Alcohol Experiments. Zeolite samples used in alcohol-quenching experiments were prepared by vapor-phase adsorption of the neat alcohol in dry zeolite/dimethoxybicumene composites. This typically involved introducing the liquid alcohol in microliter increments with a syringe through the top of a sealed laser cell containing a small quantity (ca. 100−200 mg) of the composite. The laser cell was then heated slightly with a low-temperature heat gun to vaporize the alcohol and the material was shaken to thoroughly mix the contents. The sample was allowed to cool to room temperature before conducting the laser experiments.

Product Studies. Steady-state photolyses were conducted by irradiating 4,4′-dimethoxybicumene in NaY in a sealed quartz cell under a continuous flow of either dry nitrogen or argon for periods of 72−96 h. The light source was a medium-pressure 450 W mercury lamp passed through a quartz filter. Following the photolysis small amounts of methanol (typically 100−200 μL) were injected into the irradiation cell and heat vaporized. The resultant products were separated from the zeolite by continuous extraction with dichloromethane for 24−48

(105) Kratt, G.; Beckhaus, H. D.; Lindner, H. J.; Ruchardt, C. *Chem. Ber.* **1983**, *116*, 3235−3263.

(106) Refa Nutaitis, C. F.; Bernardo, J. E. *Synth. Commun.* **1990**, *20*, 487−493.

h. The photochemical conversion was consistently about 10%, while the mass balance varied slightly between 40 and 60%. The extracts were analyzed by a combination of GC, GC/MS, and HPLC, and the products were identified by comparison to known standards.

Time-Resolved Diffuse Reflectance. Time-resolved diffuse reflectance experiments were carried out using a nanosecond laser system. The excitation source was the fourth harmonic (266 nm, <8 mJ, <8 ns/pulse) from a Continuum NY61-10 YAG laser. A Lambda-Physik excimer laser (308 nm, <100 mJ, 10 ns/pulse) was used as the excitation source in the photosensitizer experiments. The transient signals from the monochromator-PMT detection system were captured using a Tektronix 620 digitizer and then transferred via a GPIB interface to a Power Macintosh 7100 computer which controls the laser system using a program written with LabView 3.0 software. The experimental setup for time-resolved diffuse reflectance is similar to that described in detail previously.[20] The samples were contained in quartz cells constructed with 3×7 mm^2 tubing and were either evacuated under reduced pressure (10^{-3} Torr) and sealed or purged with oxygen for a minimum of 20 min prior to photolysis. The data analysis was based on the fraction of reflected light absorbed by the transient (reflectance change $\Delta J/J_o$) where J_o is the reflectance intensity before excitation and ΔJ is the change in the reflectance after excitation.

Acknowledgment. We gratefully acknowledge the Natural Science and Engineering Research Council of Canada (NSERC) and Dalhousie University for financial support of this research. M.A.O. is the recipient of an NSERC graduate scholarship and F.L.C. is the recipient of an NSERC-WFA.

Supporting Information Available: Figures S1−S4 of spectral and rate data (PDF). This material is available free of charge via the Internet at http://pubs.acs.org.

JA993619D